Dalton Transactions

Nickel oxide thin film from electrodeposited Nickel sulfide thin film: Peroxide sensing and photo-decomposition of phenol

Journal:	*Dalton Transactions*
Manuscript ID:	DT-ART-06-2014-001658.R1
Article Type:	Paper
Date Submitted by the Author:	02-Jul-2014
Complete List of Authors:	Jana, Sumanta; Bengal Engineering and science University, Department of Chemsitry Samai, Shubhasis; University of Calcutta, Department of Chemsitry Mitra, Bibhas; Bengal Engineering and science University, Department of Physics Bera, Pulakesh; Panskura Banamali College, Department of Chemsitry Mondal, Anup; Bengal Engineering and Science University, Department of Chemistry

Table of Contents

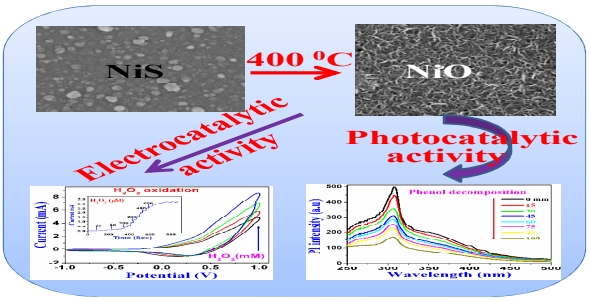

Porous NiO thin film: a peroxide sensor and effective catalyst for phenol decomposition.

Nickel oxide thin film from electrodeposited Nickel sulfide thin film: Peroxide sensing and photo-decomposition of phenol

Sumanta Jana[a], Subhasis Samai [b], Bibhas C. Mitra [c], Pulakesh Bera [d], Anup Mondal [a*]

[a] Department of Chemistry, Bengal Engineering and Science University, Botanic Garden, Howrah 711103, WB, India

[b]Department of Chemistry, University of Calcutta, 92 APC Road, Kolkata-700009

[c] Department of Physics, Bengal Engineering and Science University, Botanic Garden, Howrah 711103, WB, India

[d] Department of Chemistry, Panskura Banamali College, Vidyasagar University, Purba Medinipur, 721152, WB, India

*corresponding author email: anupmondal2000@yahoo.co.in (AM), sumantajana85@gmail.com (SJ), fax: 91-33-2668-2916

Abstract

A novel non-enzymatic peroxide sensor has been constructed by using nickel oxide (NiO) thin films as sensing material, which were prepared by two step process: (i) electrodeposition of nickel sulfide (NiS), (ii) thermal air oxidation of as-deposited NiS to NiO. The resulting material is highly porous and comprising interconnected nanofibers. UV–Vis, FTIR, X-ray photoelectron spectroscopy (XPS), X-ray diffraction (XRD) and field emission scanning electron microscope (FESEM) were used for a complete characterization of nanostructured NiO thin films. Cyclic voltametry study shows that NiO/ITO electrode facilitates the oxidation of hydrogen peroxide and exhibits excellent catalytic activity towards its sensing. The amperometric study of NiO/ITO was carried out to determine sensitivity, linear range, detection limit etc. of the proposed sensor. The sensor exhibits prominent electrocatalytic activity toward the oxidation of H_2O_2 with wide linear range and low detection limit. It has also been mentioned that the synthesized NiO thin films could be used as an effective photocatalyst for the decomposition of phenol.

Introduction

Shape and size controlled synthesis of low-dimensional electrochromic nanomaterials has become an advance research topic due to its wide applications in different fields of science and technology.[1,2] The device application of electrochromic material is creditable due to its efficient electron transport property.[3] Nickel oxide (NiO), an electrochromic material (band gap energy from 3.6 to 4.0 eV) with high electron transport property, has received a great deal of interest because of its versatile application in modern science and technology. Thin films of NiO are widely used as gas sensors,[4] electrochemical display devices,[5] p-type transparent conducting electrodes,[6] organic light emitting diodes (OLEDs),[7] smart windows,[8] variable reflectance mirrors and non-emissive information displays[9]. Several deposition techniques such as metal evaporation,[10] sputtering,[11] sol gel,[12] electrochemical, chemical[13] are employed to synthesize NiO thin films. However, electrochemical is a facile and controllable technique for tailoring crystallinity, morphology through several competing factors.[13] The application of the material is strongly shape, size and morphology dependent. So far, NiO nanostructures with different morphologies such as nanoplates, nanotubes, nanopowders were synthesized and used extensively in different fields.[14,15] Evans et al.[16] reported that a specific morphology of NiO e.g nanofibres is really very important nanostructure from the application point of view. In the literature, it has also been found that nickel or nickel-based chemically modified electrodes (e.g. nickel-hexacyano ferrates, hydroxides and complex modified nickel-electrodes) of a specific morphology were extensively used for the electro oxidation and reduction processes.[17-19] In this work, we have carefully investigated the synthesis of NiO thin films from electrodeposited NiS thin films. Electrocatalytic activity

of synthesized films (NiO) have been tested for peroxide sensing. Sensitivity, linear range and detection limit are calculated from amperometric analysis. The effect of pH and temperature (T) on the sensitivity was also investigated. We have shown another important application of the synthesized thin films i.e phocatalytic activity to decompose toxic phenol at an ambient temperature. Photocatalysis is an important technique for the treatment of pollutants and removal of organic compounds, since it works in ambient temperature and pressure. The photocatalytic activities of the powder nanomaterials are common [20,21] and there are very few reports of thin film that can act as photocatalyst.[22] Here we have used thin films directly to study photocatalytic activity of these materials to decompose phenol. This decomposition of toxic substances by photocatalysis could be the basis of waste treatment.[23, 24]

Experimental Section

Chemicals and Reagents

Analytical grade nickel chloride ($NiCl_2.6H_2O$) and D−tartaric acid ($C_4H_6O_6$) were purchased from Merck (India). Thioacetamide (TAA), Hydrogen peroxide (H_2O_2) and other reagents were purchased from Spectrochem (India) and used as it is without further purification. Phosphate buffer solutions (0.1 M) of pH ranging from 2 to 12 were prepared by mixing stock solutions of Na_2HPO_4/NaH_2PO_4. Deionized water was used to prepare all the solutions and to rinse the electrodes.

Deposition of NiS thin films

Nickel sulfide (NiS) thin films were electrodeposited on ITO coated glass substrate (resistance 10 ohm/cm^2, surface area 2×1 cm^2) at room temperature (25°C) using standard three electrode system (Electrochemical analyzer CHI 620D). Initially, 50 ml of

0.1 M $NiCl_2.6H_2O$ solution was mixed with 10 ml of 0.1 M aqueous solution of D−tartaric acid and stirred for 20 minutes. Then 25 ml of 0.1 M thioacetamide (TAA) solution was added and stirred for additional 10 minutes to make the working solution. The final volume of the solution was adjusted to 100 mL with deionized water. The pH of this working solution was maintained at 5.5 by adding dilute ammonia solution. A properly cleaned ITO glass substrate (working area 2×1 cm^2), a Pt foil and a saturated Ag-AgCl electrode were taken as working, counter and reference electrodes respectively. Chronoamperometric (CA) analysis was carried out to deposit NiS thin films. The CA analysis was carried out at three different potentials, viz., −0.80 V, −0.90 V and −1.00 V, respectively for 300 sec. The current-time curves of NiS thin films in the working solution (as mentioned above) at different potentials are displayed in Figure1. There is a rapid current drop at the beginning and then the current density increases and become stationery after about 150 sec. The rapid decay is due to double layer charging/discharging. Nevertheless, the current density for the thin films deposited at −0.90 V is higher than that of −1.0 V which reveals better stability of the films deposited at this potential (−0.90 V). The best stability of the material at −0.90 V was also confirmed from its physical appearance. Out of the three deposition potentials studied, it was observed that uniform, stable and well adhered films were obtained only at −0.90 V (though current density at −0.80 V is maximum, but the deposited material was not well adhered to the ITO substrate). The synthesized, well adhered black films were washed thoroughly with water and methanol. Optical analysis and EDAX of as deposited NiS have been incorporated in supplementary information (SI).

As deposited NiS thin films were thermally oxidized at 300°C, 400°C and 450°C for 20 minutes to generate oxide films. The black NiS transferred to cloudy white NiO upon air oxidation.

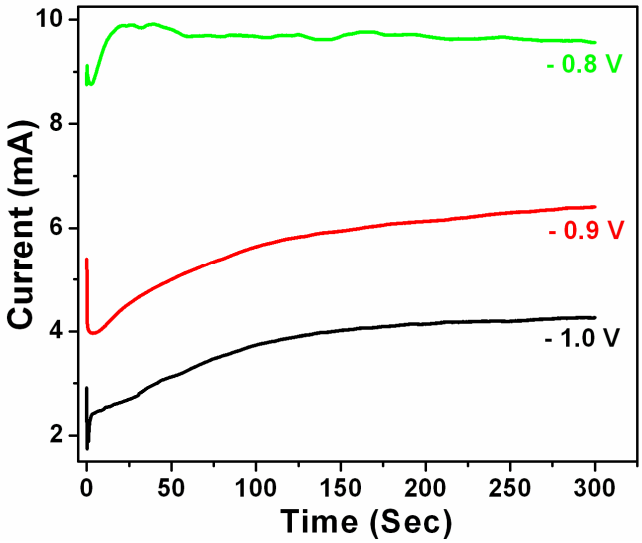

Figure 1: Chronoamperometric (CA) deposition of NiS on ITO substrate at −0.8 V, −0.9 V and −1.0 V, in presence of $NiCl_2$. $6H_2O$ (50 ml 0.1 M), D−tartaric acid (10 ml 0.2 M) and 25 ml of 0.1 M thioacetamide (TAA) solution at pH 5.5.

Physical measurements

The structural properties of the thin films were studied by X-ray diffraction (XRD) with a Seifert P3000 diffractometer using Cu Kα (λ = 1.54 A°) radiation over an angle of 20^0 to 80^0. The surface microstructure and morphology were analyzed with a Gemini Zeiss Supra 35VP (Carl Zeiss Microimaging GmbH, Berlin, Germany) Field Emission Scanning Electron Microscope (FESEM). The optical properties were recorded by UV-Vis (JASCO V-530) and FTIR (JASCO FTIR-460) spectrophotometers. X-ray photoelectron spectroscopy (XPS) measurement was carried out on an ESCLAB KMII

using Al as the exciting source and photoluminiscence (PL) spectra were recorded with Perkin–Elmer LS-55 Fluoremeter.

Electrocatalytic study

The electrochemical oxidation and amperometric detection of H_2O_2 by NiO/ITO electrodes (active area = 2×1 cm^2) were monitored in a standard three electrode system. In the electrochemical cell set up, NiO/ITO thin film was taken as a working electrode, a platinum wire and an Ag/AgCl electrode were used as auxiliary and reference electrodes respectively. Cyclic voltammograms (CVs) were recorded in a cell containing 20 mL of 0.1 M phosphate buffer (pH 9.0, 50°C) with a scan rate of 0.1 V s^{-1}. Same cell setup was used at a constant potential 0.50 V (vs. Ag/AgCl) for amperometric measurement.

Results and Discussion

Figure 2 (a) represents the X-ray diffraction pattern of electrodeposited NiS thin film (deposited at −0.90 V) on ITO substrate. Comparing the observed diffraction pattern with standard JCPDS, it was found that the peak values (2θ) as well as intensity matched well with the JCPDS card no. 12-0041. The pattern shows three major diffractions from (300), (021), and (131) planes, corresponds to rhombohedral NiS (a = 9.620 Å, c= 3.149 Å, Z = 9, C = 0.3273). Presence of free Ni, NiO or other intermediate phases of NiS was not detected in the XRD pattern.

Figure 2 (b) shows the XRD pattern of NiS film, annealed at 300°C. A mixed phase of NiS-NiO was generated. The observed and standard values, along with (h k l) planes are in good agreement with JCPDS # 04-0835. The pattern shows two major diffractions from (111) and (200) planes correspond to the cubic structure of NiO. Two additional diffraction peaks (corresponding to the planes (300) and (131)) with diminished intensity,

in the spectrum are due to the presence of parent NiS with the newly formed NiO. Hence, annealing at 300°C results in incomplete conversion of NiS to NiO. Pure phase of NiO was detected at relatively higher temperatures e.g., 400°C and 450°C which is confirmed from Figure 2 (c) and (d). The figures (Figure 2 (c) and (d)) represent the XRD patterns of NiS thin films annealed at 400°C and 450°C, respectively. The observed patterns were compared with standard JCPDS data and found to match well with JCPDS 04-0835 for cubic NiO. Here, the parent peaks of NiS were not detected, which indicates total conversion of NiS to NiO at this temparetures. The observed d values, along with (h k l) indexed planes are in good agreement with standard d values. The peaks marked '*' in the XRD pattern appears due to the In_2O_3 present in the ITO substrate [JCPDS ID 44-1087].

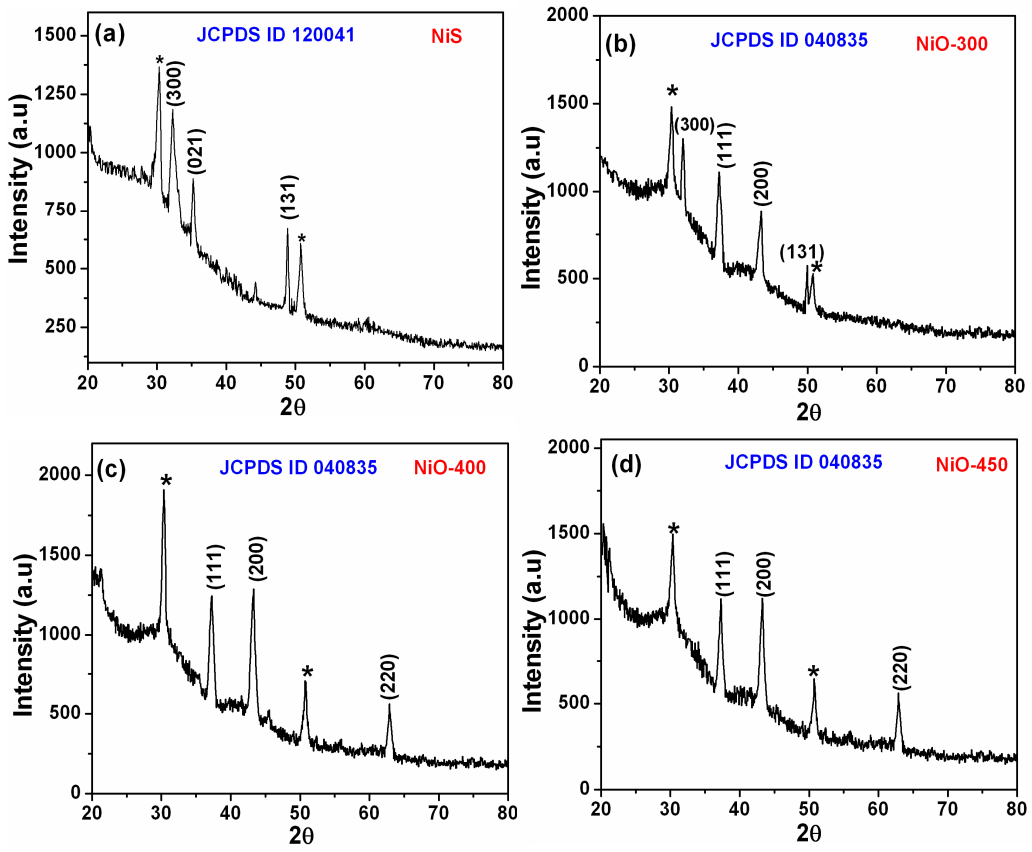

Figure 2: XRD patterns of (a) as deposited NiS (b) NiS thin film annealed at 300°C (horizontal planes (131),(300) are of NiS) (c) NiS thin film annealed at 400°C (d) NiS thin film annealed at 450°C.

Figure 3(a) shows the FESEM image of as deposited NiS. Nearly spherical clusters were grown over the ITO substrate. Discrete surface coverage with randomly distributed spherical nano clusters is evident from the SEM image.

Figure 3 (b) represents the SEM image of NiS thin film annealed at 300°C. An enormous morphological change is clearly visible from this SEM image. Clusters of NiS get fused and form a flaky homogeneous morphology due to air oxidation. Good coverage of the ITO surface by the material is also evident from the SEM image. Figure 3 (c) represents the SEM image of NiS thin film annealed at 400°C. Here, the new generated morphology is very interesting. The entire ITO surface is fully covered with uniformly distributed NiO fibers. Morphology of the deposited material is highly porous and composed of interconnected nano fibers. This uniform and high order porous morphology is very important from the application point of view. Figure 3 (d) shows the SEM image of 450°C annealed NiS thin film. Totally agglomerated cluster type morphology is evident from the SEM image. Hence, from the SEM study it is clear that annealing temperature is the key factor for morphological changes, but higher temperature does not necessarily assure better morphology of the nanostructured films. From the morphological investigation it can be concluded that the material developed at 400°C is interesting and can be used in potential application. Therefore it is selected for the following characterizations and is used for the application purpose. The following characterizations We have tried several times to scrap off NiO powder from the ITO surface, but the

synthesized material (NiO) was so strongly adhered to ITO that we were unable to collect a minimum amount of powder material for BET and HRTEM analysis.

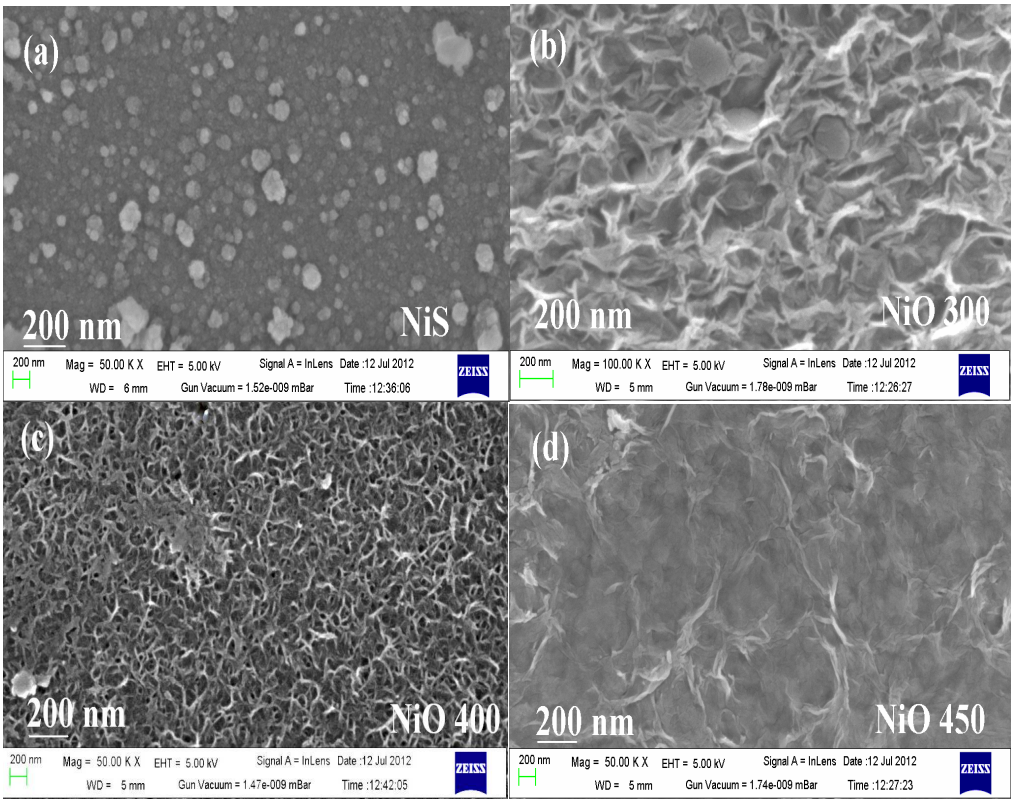

Figure 3: FESEM images of (a) NiS thin film (b) NiS thin film annealed at 300°C (C) NiS thin film annealed at 400°C (d) NiS thin film annealed at 450°C.

The optical properties of the films were recorded using UV–Vis and FTIR spectrophotometry. As displayed in Figure 4(a), the absorption spectrum shows a sharp onset in absorbance at around 400 nm. The band gap energy was calculated using Tauc's relation: $(\alpha h\nu)^{1/n} = A(h\nu - E_g)$ where, hν is the incident photon energy, 'A' is a constant and 'n' is the exponent, the value of which is determined by the type of electronic transition causing the absorption and can take the values 1/2 or 2 depending upon

whether the transition is direct or indirect, respectively. Since, NiO is a direct band gap semiconductor, we can evaluate E_g from the plot of $(\alpha h\nu)^2$ vs. hν. The inset of Figure 4 (a) shows the $(\alpha h\nu)^2$ vs. hν plot, corresponding to band gap 3.65 eV. This band energy was calculated considering the thickness of NiO thin film to be 280 nm which has been confirmed from surface Profilometer (Bruker Contour GT).

FTIR (400 to 3000 cm^{-1}) spectrum of NiO thin film (Figure 4(b)) shows only one sharp band at 553 cm^{-1}. This represents the stretching of Ni-O, which is in agreement with similar observation by Korosec et al.[25] Presence of no other peaks in the spectrum clearly indicates the absence of water molecules and /or hydroxide ions. Optical analysis and other characterizations of NiS have been incorporated in Supplementary material.

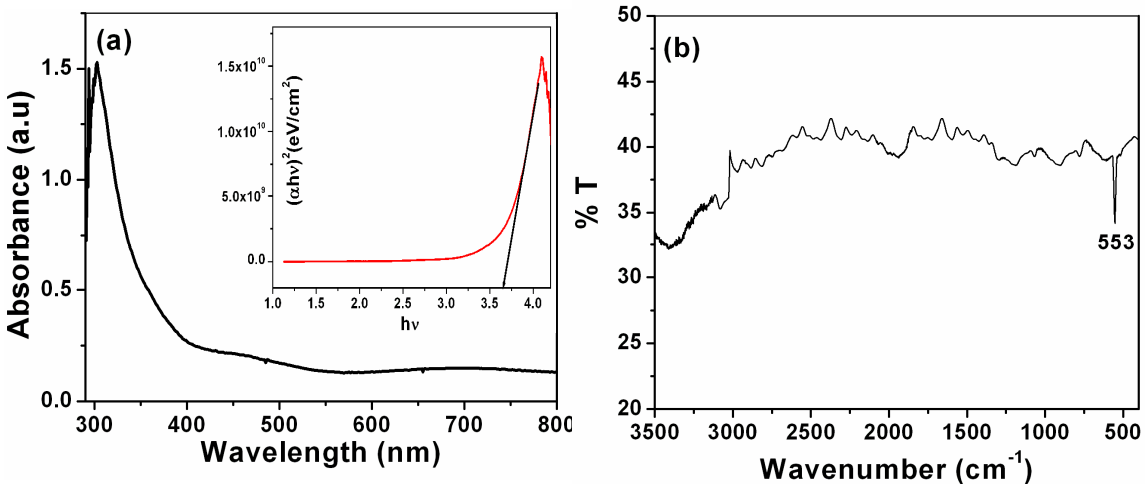

Figure 4: (a) UV-Vis spectrum of NiO, inset Tauc plot (b) FTIR spectrum of NiO thin film.

The XPS measurement reveals the chemical states of bonded atoms. Figure 5(a) and 5(b) are the XPS spectra of deposited NiO for the Ni 2p and O 1s. XPS spectrum of Ni^{2+} (Figure 5(a)) shows two peaks at binding energies 852.3 eV and 872.01 eV

corresponding to Ni $2p_{3/2}$ and Ni$2p_{1/2}$ states. The spectrum suggests only the presence of +2 state of Ni. Whereas, the peak centered at 530.8 eV corresponds to the O 1s (Figure 5(b)) which indicates a normal state of O^{2-} in the compound.

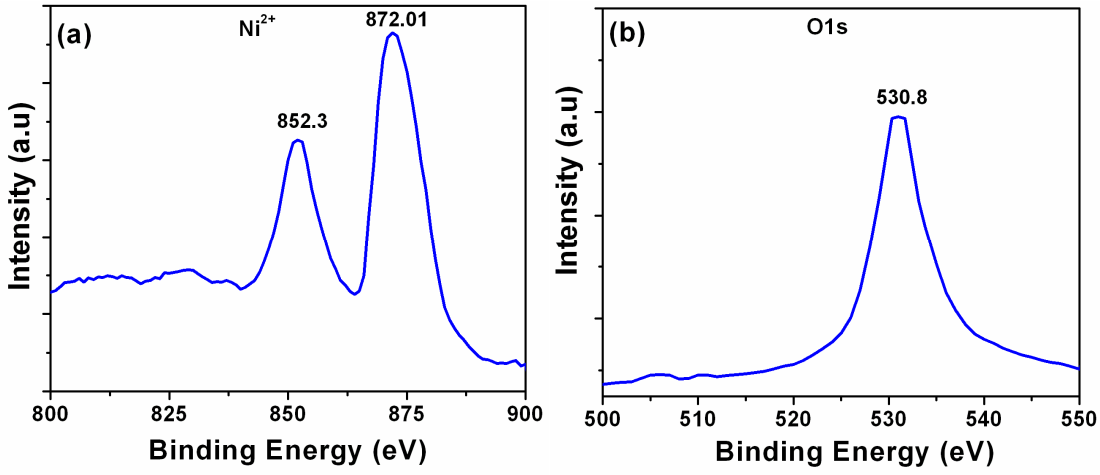

Figure 5: XPS spectra of NiO thin film

Electrocatalytic activity of NiO

The electrocatalytic activities of NiO/ITO thin films were explored by cyclic voltametry (CV) study. Being a frequent product of many enzymatic reactions catalyzed by a large number of oxidases, H_2O_2 was taken as a model molecule in the field of biosensor.[26] Cyclic voltammograms (CVs) were recorded in a cell containing 20 mL of 0.1 M phosphate buffer (PBS) at pH 9.0 with gradual addition of H_2O_2 (mM). The same cell setup was used at constant applied potential 0.50 V (vs. Ag/AgCl) for chronoampermetric (CA) measurement. The amperometric responses were recorded with successive H_2O_2 addition (μM range) into the PBS buffer. The apparent Michaelis–Menten constant K_M^{app} and the maximum current for NiO/ITO electrode were determined using the Michaelis–Menten equation.[27]

$$I = (I_{max} \times [S]) / (K_M^{app} + [S]) \quad (i)$$

Where, I is the steady-state current, I_{max} is the maximum current measured under enzyme saturation, [S] is the concentration of substrate. Rearrangement of Michaelis–Menten equation yields the electrochemical version of the Lineweaver–Burk equation, which also enables the analysis of the enzyme kinetics.

$$1 / I = 1/ I_{max} + K_M^{app} / (I_{max} \times [S]) \quad (ii)$$

Performance of NiO thin film towards oxidation of H_2O_2

Figure 6 represents the CV's of NiO/ITO electrode in PBS buffer at pH 9.0 at a scan rate of 0.1 V s^{-1}. The first CV scan was taken without adding H_2O_2 into the buffer solution and at 0.50 V an oxidation peak was detected. Then H_2O_2 was gradually (mM range) added to this PBS buffer and the oxidation peak (at 0.50V) increases with gradual addition of H_2O_2. This increase in current height (in anodic sweep) with gradual addition of H_2O_2 indicates an obvious electrocatalytic oxidation of H_2O_2. The oxidation potential was found to be around 0.50 V, compared to 0.60 V for CPE (carbon paste electrode) modified Nickel oxide electrode.[28]

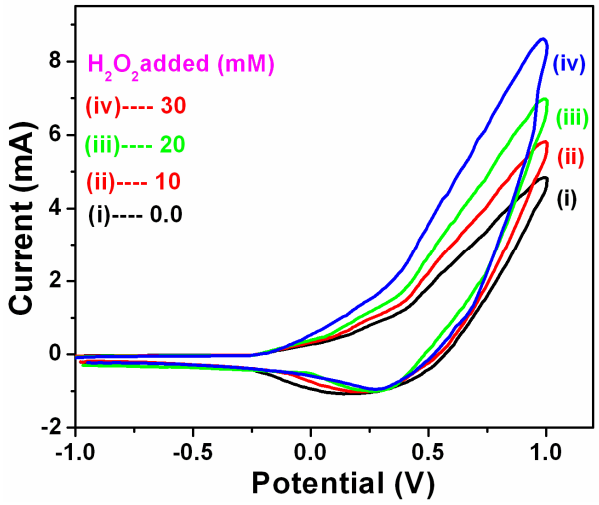

Figure 6: CV's of NiO/ITO electrode in phosphate buffer solution (PBS, pH 9) with different amount of H_2O_2 addition.

In order to check the amperometric H_2O_2 sensor activity, the current response with concentration of H_2O_2 at working potential i.e 0.5 V was studied and has been shown in Figure 7. When an aliquot amount of H_2O_2 (μM range) was added to the PBS buffer, the oxidation current rises sharply and then reaches a steady value within 10 s. The response time of the sensor was 10 s and the attainment of steady state current was an additional 4 s. But for NiS/ITO electrode no catalytic response was observed.

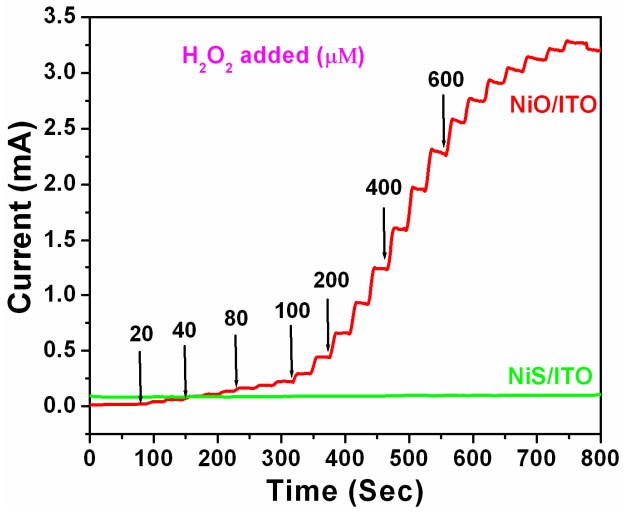

Figure 7: Amperometric responses of NiS/ITO and NiO/ITO electrodes with successive addition of H_2O_2 to PBS at an applied potential of 0.50 V (vs. Ag/AgCl).

To obtain calibration curve, the steady state current values were plotted against the concentration of H_2O_2 and shown Figure 8(a). The calibration curve shows that with addition of H_2O_2, the current increases linearly and it reaches to a steady state after a certain period. From the calibration curve, the linear region was estimated and found to

10 μM–1000 μM. The calibration curve was also used to calculate the sensitivity of the proposed sensor and which was found to ~2.3 mA/mM (correlation coefficient 0.9318). The detection limit was also estimated to 1.28 mM (signal-to-noise ratio = 3).

Now, applying Lineweaver–Burk model (equation ii) on Figure 8(b), the apparent Michaelis–Menten constant (K_M^{app}) was calculated from the plot of $1/I_{cat}$ vs.1/S (Figure 8(b)). The K_M^{app} was found to around 0.65 mM. The K_M^{app} is smaller than some other electrodes like horseradish peroxidase (HRP),[29] Fe_2O_3/GC and PB-Fe_2O_3/GC.[30] The smaller K_M^{app} value suggests that the electrode has a higher affinity to oxidized H_2O_2. A comparative study of H_2O_2 sensing with other reported sensors [35–45] reveals that our NiO/ITO electrode is quite effective as a peroxide sensor (Supporting Information Table 1).

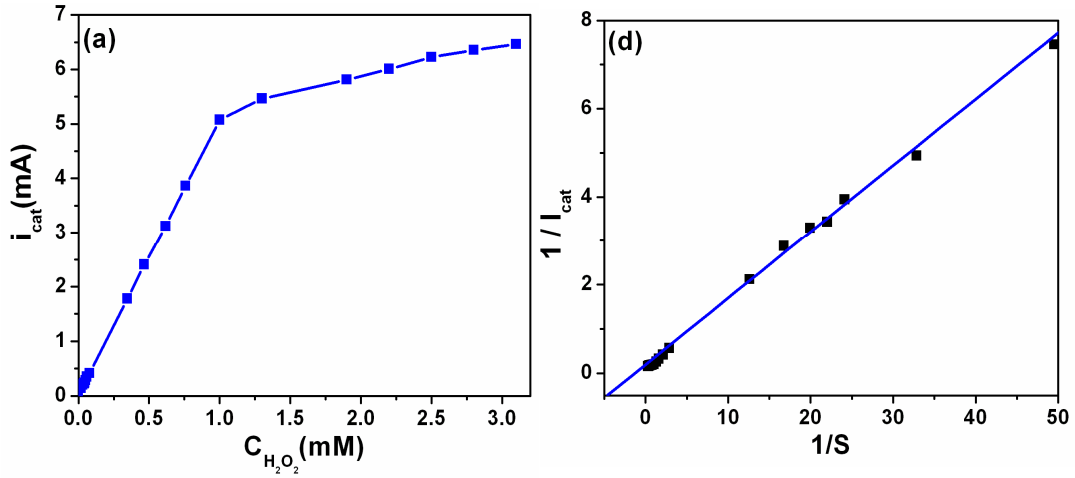

Figure 8: (a) Calibration curve (b) corresponding Lineweaver–Burk plot of of NiO/ITO electrode.

pH and temperature (T) dependent stability and sensitivity

The stability and the performances of the modified electrodes were tested over a wide range of pH (2–11) and temperature (10−80°C). It was investigated that maximum electrocatalytic decomposition of H_2O_2 took place at pH 9 (Figure 9(a)) and at 50ºC maximum catalytic activity (Figure 9(b)) was detected.

The reproducibility and stability of this NiO/ITO based new sensor were also studied by adding a fixed amount of H_2O_2 (1 mM) to the buffer solution. The relative standard deviation (RSD) of the sensor response was 4.7% for five successive measurements using the same electrode. The NiO/ITO electrode activity was restored up to 90% on storing the electrode at 20°C for 20 days which suggests the long-term stability of the electrode.

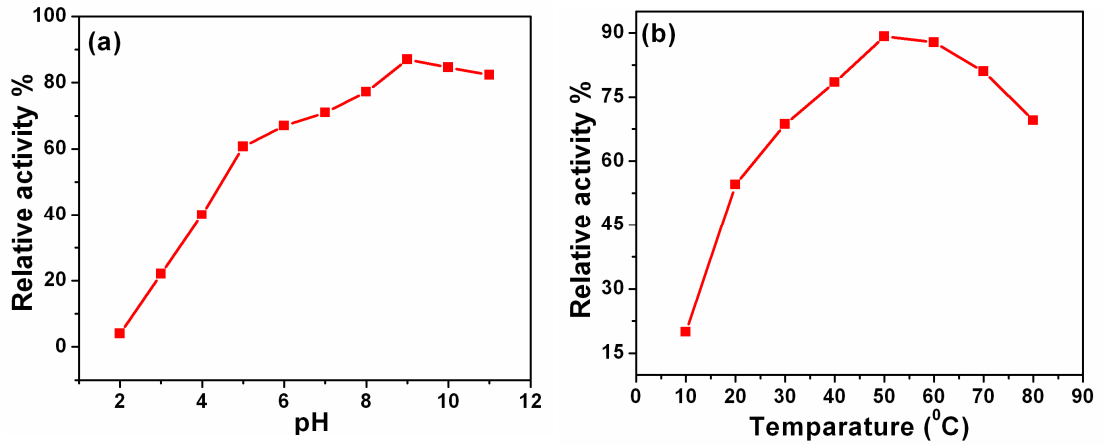

Figure 9: Effect of (a) pH and (b) temperature (T) for the catalytic response of NiO/ITO electrode towards H_2O_2 sensing.

Photodegradation of phenol

To demonstrate the potential applicability of the synthesized nanoporous NiO thin films, we investigated its relative activity with phenol degradation. Phenol is a major pollutant of surface and groundwater and according to WHO's recommendation in 1994 (World

Health Organization) the exposure limit of phenol in inland water should not be higher than 0.02 mg/ L.[31]The secure level degradation within this range is really difficult due to its stability and solubility in water. In the present work we have investigated the phocatalytic activity of the synthesized materials (NiO), taking directly the thin films (as the scrapping off NiO powder material from ITO substrate is not possible due to well adherence of NiO with ITO substrate). Five same size thin films of active surface area 2×1 cm^2 were vertically placed into a 100 ml (100 ppm) aqueous solution of phenol. At specific time intervals (15 minutes), aliquot amount of phenol was withdrawn from the reaction bath and the changes in concentration were monitored with PL spectroscopy, at an excitation of 280 nm. From Figure 10 (a) it is clear that maximum emission occurs at ~307 nm which is the characteristic fluorescence emission of phenol (λ_{max} value of pure phenol was determined by Uv-Vis spectroscopy and was found to be 258 nm). It has been observed that the intensity decreases gradually with increasing exposure time. Figure 10 (b) represents the relative conc. vs time plot which says that the emission peak intensity decreases up to 66 % within 100 minutes. The decrease of the emission peak intensity at 307 nm is attributed to the degradation of phenol. Hence our synthesized NiO thin films show effective photocatalytic reactivity in the decomposition of phenol. The essential requirement for phenol decomposition is separation of electrons (e^-) and holes (h^+) by absorbing light. The photo generated electrons and holes react with adsorbed surface substances, like O_2, OH^- and form reactive species O_2^-, OH* (hydroxyl radicals). These are the major oxidative species for the decomposition of organic pollutants. Degradation of phenol corresponds to hydroxylation of the phenyl ring as promoted by hydroxyl radicals (·OH) [32] where excited NiO nanoparticles get the necessary activation energy to

react with ·OH radicals and produce CO_2 and H_2O.[33] The common intermediates viz., catechol, hydroxyhydroquinone, hydroquinone, benzoquinone etc. are also expected to form during the decomposition.[34] A Possible photodegradation mechanism of phenol is illustrated in Figure 11

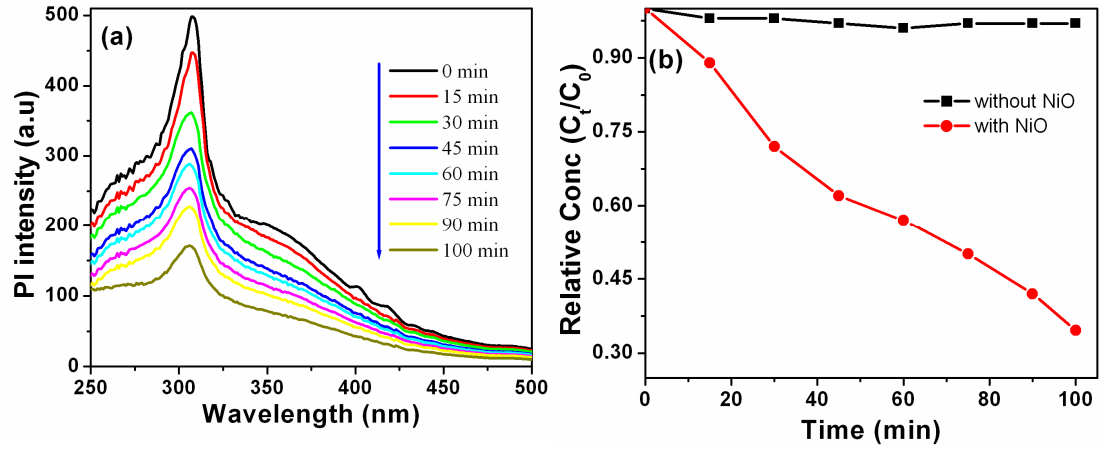

Figure 10: (a) Photoluminescence spectra of residual phenol in presence of NiO thin films at an excitation wavelength at 280 nm (b) Intensity of residual phenol as a function of irradiation time.

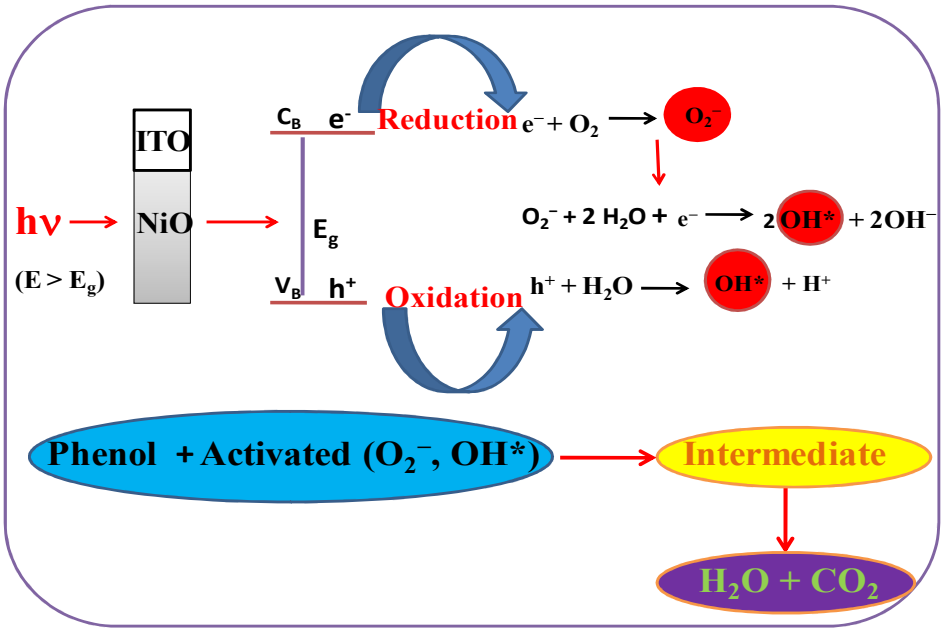

Figure 11: Schematic representation of possible photodegradation path.

Conclusion

Nano-sized NiO thin films were successfully synthesized by the oxidation of electrodeposited NiS thin films at 400 °C. Electrodeposition of nickel sulphide and their conversion to nickel oxide thin films by air annealing are found to be a convenient cost-effective method. The synthesized NiO thin films were found to be effective towards H_2O_2 oxidation. High sensitivity and wide linear range features make it as an effective sensor. pH and temperature dependent study suggests that the catalytic activity is strongly dependent on these parameters. Reproducibility and stability study also reveals long-term stability of the sensor. The synthesized NiO thin films show high photocatalytic activity towards decomposition of phenol. The result indicates a great potential application of NiO as pollutant cleanup for environmental interest.

Acknowledgements

The author S. Jana is thankful to University Grants Commission (UGC), Government of India, for providing him Research Fellowship (Ref. No. 20-12/2009 (ii) EU-IV). The authors acknowledge DST-SERI (India) for the Electrochemical Analyzer and U.G.C.-S.A.P (India) for providing other instrumental facilities to the Department of Chemistry, IIEST, Shibpur.

References

1 C. Burda, X. Chen, R. Narayanan and M.A. El-Sayed, *Chem. Rev.,* 2005, **105,** 1025–102.

2 M-C Daniel and D. Astruc, *Chem Rev.,* 2004, **104,** 293–346.

3 A.K Wanekaya, W. Chen, N.V. Myung and A. Mulchandai, *Electroanalysis,* 2006, **18,** 533–550.

4 I. Hotovy, J. Huran, P. Siciliano, S. Capone, L. Spiess and V. Rehacek, *Sens. Actuators B,* 2001, **78,** 126–132.

5 M. Kitao, K. Izawa, K. Urabe, T. Komatsu, S. Kuwano and S. Yamada, *Jpn. J. Appl. Phys.,* 1994, **33,** 6656–6662.

6 H. Sato, T. Minami, S. Takata and T. Yamada, *Thin Solid Films,* 1993, **236,** 27–31.

7 I. M. Chan, T.Y. Hsu and F.C. Hong, *Appl. Phys. Lett.,* 2002, **81,** 1899–1901.

8 P.C. Yu and C.M. Lampert, *Sol. Energy Mater.,* 1989, **19,** 1–16.

9 J.S.E.M. Svensson and C.G. Granqvist, *Sol. Energy Mater.,* 1985, **12,** 391– 402.

10 J.S.E.M. Svensson and C.G. Granqvist, *Sol. Energy Mater.,* 1987, **16,** 19–26.

11 A.E. Jiménez-González, J.G. Cambray and A.A.R. Gutiérrez, *Surface Engineering,* 2000, **16,** 77–79.

12 W. Brückner, R. Kaltofen, J.Thomas, M. Hecker, M. Uhlemann, S. Oswald, D. Elefant and C.M. Schneider, *J. Appl. Phys.,* 2003, **94,** 4853 – 4858.

13 L. Berkat, L. Cattin, A. Reguig, M. Regragui and J.C. Bernede, *Mater. Chem. and Phys.,* 2005, **89,** 11–20.

14 Y.G. Wang and Y.Y. Xia, *Electrochim Acta.,* 2006, **51,** 3223 – 3227.

15 G. Malandrino, L.M.S. Perdicaro, I.L. Fragal, R.L. Nigro, M. Losurdo and G. Bruno, *J. Phys. Chem. C,* 2007, **111**, 3211–3215.

16 S.A.G. Evans, J.M. Elliott, L.M. Andrews, P.N. Bartlett, P.J. Doyle and G. Denuault, *Anal. Chem.,* 2002, **74,** 1322–1326.

17 A. Kicela and S. Daniele, *Talanta,* 2006, **68,** 1632–1639.

18 S. Majdi, A. Jabbari and H. Heli, *J. Solid State Electrochem.,* 2007, **11,** 601–607.

19 M. Jafarian, M. G. Mahjani, H. Heli, F. Gobal and M. Heydarpoor, *Electrochem. Commun.,* 2003, **5***,* 184 –188.

20 Y. Zheng, C.Chen, Y. Zhan, X.Lin, Q.Zheng, K.Wei, J.Zhu and Y.Zhu, *Inorg.Chem.,* 2007, **46,** 6675 –6682.

21 J. Wang, P. Liu, X. Fu, Z. Li, W. Han and X. Wang, *Langmuir,* 2009, **25,**1218–1223.

22 M. Bizarro, *Appl. Catal. B,* 2010, **97,**198–200.

23 S. Ahmed, M.G. Rasul, W. N. Martens, R. Brown and M.A. Hashib, *Desalination,* 2010, **261,** 3–18.

24 S.L. Koro and L. Dekany, *Colloids Surf. A*, 2006, **280,** 146–154.

25 R.C. Korosec, P. Bukovec, B. Pihlar, A.S. Vuk, B. Orel and G. Drazic, *Sol. St. Sci.,* 2003, **191,** 191–200.

26 A. Salimi, R. Hallaj, S. Soltanian and H. Mamkhezri, *Anal. Chim. Acta.,* 2007, **594,** 24– 31.

27 R.A. Kamin and G.S. Willson, *Anal. Chem.,* 1980, **52,** 1198–1205.

28 R.Ojani, J.B. Raoof and B. Norouzi. *Int. J. Electrochem. Sci.,* 2012, **7,**1852–1863.

29 J. Li, S.N. Tan and H. Ge, *Anal. Chim. Acta,* 1996, **335,** 137–145.

30 A. Dutta, S.K. Maji, D.N. Srivastavab, A. Mondal, P. Biswas, P. Paul and B. Adhikary, *J. Mol. Catal. A: Chem.,* 2012, **360,** 71–77

31 D. Wang, C. Song, Z. Hu and X. Fu, *J. Phys. Chem. B,* 2005, **109,** 1125 –1129.

32 T. Zhu, J. S. Chen and X. W. (David) Lou, *J. Phys. Chem. C,* 2012, **116,** 6873–6878.

33 D. Li and H. Haneda, *Chemosphere,* 2003, **51,** 129–137.

34 A. Sobczynski, L. Duczmal and W. Zmudzinski, *J. Mol. Catal. A: Chem.,* 2004, **213,** 225–230.

35 M. ElKaoutit, I.N. Rodriguez, M. Dominguez, M.P.H. Artiga, D.B. Milla and J.L.H. Hidalgo de Cisneros, *Electrochim. Acta.,* 2008, **53,** 7131–7137.

36 H. Ju, S. Liu, B. Ge, F. Lisdat and F.W. Scheller, *Electroanalysis,* 2002, **14,** 141–147.

37 C.Y. Lin, Y.H. Lai, A. Balamurugan, R. Vittal, C.W. Lin, K.C. Ho, *Talanta,* 2010, **82,** 340 –347.

38 C. Xiang, Y. Zou, L.X. Sun and F. Xu, *Sens. Actuators B,* 2009, **136,** 158 –162.

39 L. Zhang, Z. Fang, Y.Ni and G. Zhao, *Int. J. Electrochem. Sci.,* 2009, **4,** 407– 413.

40 X. Bo, J. Bai, L. Wang and L. Guo, *Talanta,* 2010, **81,** 339–345.

41 W. Jia, M. Guo, Z. Zheng, T. Yyu, E.G. Rodriguez, Y. Wang and Y.J. Lei, *Electroanal. Chem.,* 2009, **625,** 27– 32.

42 Z. Dai, S. Liu, J.Bao and H. Ju, *Chem. Eur. J.,* 2009, **15,** 4321– 4326.

43 X. Xu, S. Jiang, Z.Hu and S. Liu, *ACS Nano,* 2010, **4,** 4292–4292.

44 J.C. Ndamanisha, Y. Hou, J. Bai and L. Guo, *Electrochim. Acta.,* 2009, **54,** 3935–3942.

45 A. Mehta, S. Patil, H. Bang, H.J. Cho and S. Seal, *Sens. Actuators A,* 2007, **134,** 146–151.